# Backside-gate-assisted Broadband Modulation on Silicon-polymer Hybrid Photonic Crystal Waveguide

[1,5]Xingyu Zhang*, [2]Amir Hosseini, [2]Harish Subbaraman, [3]Jingdong Luo, [3]Alex A.K. Jen,
[1]Chi-jui Chung, [1]Hai Yan, [1]Zeyu Pan, [4]Robert L. Nelson, and [1,2]Ray T. Chen*
[1]Microelectronics Research Center, Electrical and Computer Engineering Department, University of Texas at Austin, Austin, TX, 78758, USA
[2]Omega Optics, Inc., Austin, TX 78759, USA
[3]Department of Materials Science and Engineering, University of Washington, Seattle, Washington 98195, USA
[4]Air Force Research Laboratory at Wright Patterson, Dayton, Ohio 45433, USA
[5]Now with Hewlett-Packard Laboratories, 1501 Page Mill Rd, Palo Alto, CA, 94304, USA
*Corresponding author: xzhang@utexas.edu, raychen@uts.cc.utexas.edu, Tel:512- 471-4349, Fax: +1-512-471-8575

**Abstract:** We demonstrate an electro-optic polymer filled slot photonic-crystal waveguide modulator with a record-high effective in-device $r_{33}$ of 1230pm/V. Assisted by a backside gate-field, 3-dB bandwidth of 15GHz and energy consumption of 94.4fJ/bit are experimentally demonstrated.

The combination of silicon photonics and electro-optic (EO) polymers has enabled compact and high-performance hybrid integrated photonic devices, such as modulators [1], interconnects [2] and sensors [3]. Especially, slow-light silicon photonic crystal waveguides (PCWs) filled with EO polymer further reduce the device size and enhance the device performance by combining the best of these two worlds. In this paper, we demonstrate an improved performance of a silicon-polymer hybrid PCW modulator assisted by backside gate. The $V_\pi \times L$ of the modulator is measured to be 0.282V×mm, corresponding to a record-high effective in-device $r_{33}$ of 1230pm/V. Assisted by a backside gate field of 100V/μm, the 3-dB bandwidth of the modulator is demonstrated to be 15GHz, and a modulation response up to 50GHz is observed. The energy consumption is estimated to be 94.4fJ/bit at 10Gbit/s. In addition, an 8nm-wide low-dispersion spectrum range is also demonstrated, which is 10X better than other non-band-engineered PCWs and ring resonators.

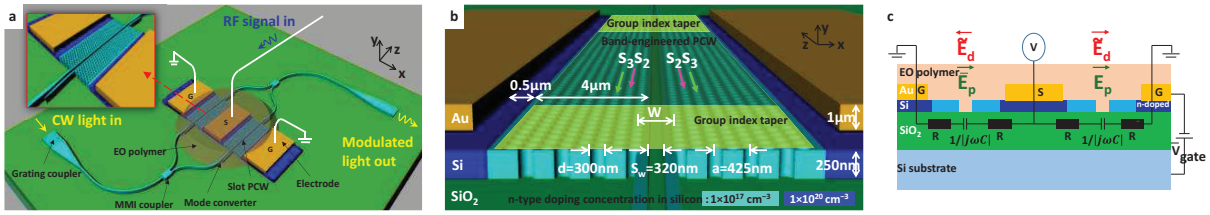


Fig. 1. (a) A 3D perspective of the an EO polymer filled silicon slot PCW MZI modulator designed on an SOI substrate. (b) A tilted view of the lattice-shifted PCWs on one arm of the MZI. (c) Equivalent electrical circuit of the MZI modulator in a push-pull configuration, with a constant gate voltage applied on the backside silicon substrate.

As shown in Fig. 1 (a), our optical modulator is a symmetric Mach-Zehnder interferometer (MZI), with 300μm-long slot PCWs incorporated in both the arms, on an SOI substrate with 250nm-thick top silicon layer and 3μm-thick buried oxide (BOX) layer. The slot PCWs are filled with EO polymer (EO coefficient, $r_{33}$=100pm/V). Mode converters and group index tapers are designed to efficiently coupled light into the slow-light PCWs [4]. Lattice-shifted PCWs are designed for a low-dispersion group index of 20.4 (±10%) over ~8nm optical spectrum range [1]. As shown in Fig. 1 (b), the silicon PCW is selectively implanted doped (n-type) to reduce the RC time delay. The modulator is driven by lumped electrodes in a push-pull configuration, as shown in Fig. 1 (c). Most importantly, a gate voltage ($V_{gate}$) is applied onto the backside silicon substrate to generate an conductive electron-accumulation layer at the interface between the silicon PCW and the BOX layer [5], leading to an enhanced RF bandwidth and a reduced energy consumption of the modulator.

The fabrication procedure starts with an SOI wafer. Silicon slot PCWs are patterned by e-beam lithography and reactive ion etching, and then selectively doped twice by photolithography and ion implantation. Gold electrodes are patterned by photolithography, e-beam evaporation, and lift-off. Next, EO polymer is spincoated to fill the slots and holes of PCWs. Finally, the EO polymer is poled at 150℃ under a constant electric field of 100V/μm in a push-pull configuration, as shown in Fig. 1 (c). The poling leakage current density is measured to be below 5.5A/m$^2$.

In the measurements, first, TE-polarized light (1550nm) is coupled into and out of the device through grating couplers, and RF signals are applied to the electrodes as shown in Fig. 1 (c). The modulator is biased at 3dB point and driven by a sinusoidal RF wave with $V_{pp}$=1.4V at 100KHz. The modulated optical signal is sent to a photodetector and displayed on an oscilloscope, as shown in Fig. 2 (a). From the over-modulation transfer function, the $V_\pi$ of the modulator is measured to be 0.94V, corresponding to $V_\pi \times L$=0.282V×mm. The slow-light enhanced effective in-device $r_{33}$ is then calculated as $r_{33-effective} = \frac{\lambda S_W}{n^3 V_\pi \sigma L} = 1230\text{pm/V}$, where, λ=1.55μm, $S_w$=320nm, n=1.63, L=300μm, σ=0.33 (confinement factor in

the slot). Discounting the slow-light effect, the actual in-device $r_{33}$ is estimated to be 98pm/V. Furthermore, the same test is repeated over the duration of a month, and no severe degradation of device performance is observed.

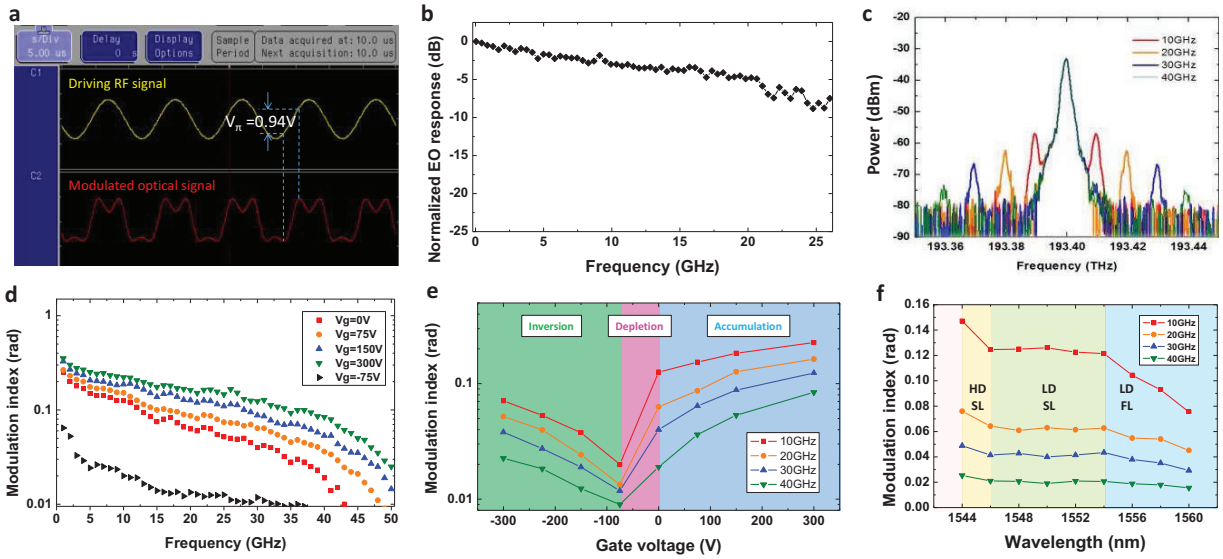


Fig. 2. (a) Over-modulation transfer function in low-frequency test. (b) Measured EO response as a function of frequency in a high-speed small-signal modulation test. (c) Measured optical transmission spectra at 10GHz, 20GHz, 30GHz and 40GHz. (d) Measured modulation index as a function of frequency, under different backside gate voltages. (e) Measured modulation index as a function of $V_{gate}$ at different frequencies. (f) Measured modulation index over a range of optical wavelengths.

Next, the RF bandwidth is measured in a high-frequency small signal modulation test. The measured EO response as a function of modulation frequency is shown in Fig. 2 (b), from which a 3-dB bandwidth of 11GHz is measured. Another test is performed using a sideband detection technique [5], and the measured optical transmission spectra of the modulator driven at different frequencies are overlaid in Fig. 2 (c). The phase modulation index (η) as a function of modulation frequency is then extracted [5] and shown by the red curve in Fig. 2 (d). Next, to further increase the RF bandwidth of the modulator, a positive gate voltage ($V_{gate}$) is applied onto the backside silicon substrate, as shown in Fig. 1 (c). As the $V_{gate}$ is increased, the measured modulation index curves become flatter [Fig. 2 (d)], due to the increased electron accumulations [5] at the interface of silicon PCWs and BOX. Under the $V_{gate}$ of 300V (i.e. $E_{gate}$=100V/μm), the 3-dB bandwidth of the modulator is increased to 15GHz, and modulation response up to 50GHz is observed. In addition, under $E_{gate}$=100V/μm, the RF power consumption for 100% modulation depth is $2\pi f \times (\frac{1}{2} CV_{\pi}^2) \times 2$=24mW. And also, the energy consumption is estimated to be $W_{bit} = \frac{1}{4} CV_{\pi}^2 \times 2$=94.4fJ/bit at 10Gbit/s [6]. Next, the $V_g$ is slightly tuned to be negative, and the measured modulation index decreases [Figs. 2 (d) and (e)] due to the depletion of electrons. As the magnitude of negative $V_g$ further increases, modulation index starts to increase because an "inversion" state occurs.

Furthermore, to demonstrate the wide low-dispersion optical bandwidth, the wavelength of the laser input is tuned and the corresponding modulation index is measured. As shown in Fig. 2 (f), at each modulation frequency, the curve of measured modulation index looks flat from 1546nm to 1554nm, with a small variation of ±3.5%. This is because the $n_g$ and slow-light enhancement has been engineered to be almost constant in this low-dispersion slow-light wavelength region [1]. This 8-nm wide optical bandwidth is 10X better than other non-band-engineered PCWs and ring resonators.

## Reference


[1] X. Zhang, A. Hosseini, J. Luo, A. K.-Y. Jen, and R. T. Chen, "Hybrid silicon-electro-optic-polymer integrated high-performance optical modulator," in SPIE Photonic West, OPTO, 2014, pp. 89910O-89910O-6.

[2] H. Subbaraman, X. Xu, A. Hosseini, X. Zhang, Y. Zhang, D. Kwong, and R. T. Chen, "Recent advances in silicon-based passive and active optical interconnects," Optics Express, vol. 23, pp. 2487-2511, 2015.

[3] X. Zhang, A. Hosseini, H. Subbaraman, S. Wang, Q. Zhan, J. Luo, A. K. Jen, and R. T. Chen, "Integrated Photonic Electromagnetic Field Sensor Based on Broadband Bowtie Antenna Coupled Silicon Organic Hybrid Modulator," Lightwave Technology, Journal of, vol. 32, pp. 3774, 2014.

[4] X. Zhang, H. Subbaraman, A. Hosseini, and R. T. Chen, "Highly efficient mode converter for coupling light into wide slot photonic crystal waveguide," Optics Express, vol. 22, pp. 20678-20690, 2014.

[5] L. Alloatti, D. Korn, R. Palmer, D. Hillerkuss, J. Li, A. Barklund, R. Dinu, J. Wieland, M. Fournier, and J. Fedeli, "42.7 Gbit/s electro-optic modulator in silicon technology," Optics Express, vol. 19, pp. 11841-11851, 2011.

[6] X. Zhang, A. Hosseini, H. Subbaraman, J. Luo, A. Jen, R. Nelson, and R. T. Chen, "Broadband low-power optical modulator based on electro-optic polymer Infiltrated Silicon Slot Photonic Crystal Waveguide," in Frontiers in Optics, 2014, p. FTu1D. 4.